

Article

Taming Microglia in Alzheimer's Disease: Exploring Potential Implications of Choline Alphoscerate via $\alpha 7$ nAChR Modulation

Anna Flavia Cantone ^{1,†}, Chiara Burgaletto ^{1,†}, Giulia Di Benedetto ^{1,2,*}, Anna Pannaccione ³, Agnese Secondo ³, Carlo Maria Bellanca ^{1,2}, Egle Augello ¹, Antonio Munafò ¹, Paola Tarro ¹, Renato Bernardini ^{1,2,‡} and Giuseppina Cantarella ^{1,‡}

- ¹ Section of Pharmacology, Department of Biomedical and Biotechnological Sciences, University of Catania, 95123 Catania, Italy; anna.cantone@phd.unict.it (A.F.C.); chiaraburg@hotmail.it (C.B.); uni318437@studium.unict.it (C.M.B.); uni365053@studium.unict.it (E.A.); antonio.munaf0.91@gmail.com (A.M.); paolatarro@hotmail.com (P.T.); bernardi@unict.it (R.B.); gcantare@unict.it (G.C.)
- ² Clinical Toxicology Unit, University Hospital of Catania, 95123 Catania, Italy
- ³ Division of Pharmacology, Department of Neuroscience, Reproductive and Odontostomatological Sciences, University of Naples Federico II, 80131 Naples, Italy; pannacio@unina.it (A.P.); agnese.secondo@unina.it (A.S.)
- * Correspondence: giulia.dibenedetto@unict.it
- † These authors contributed equally to this work.
- ‡ These authors share senior authorship.

Abstract: Alzheimer's disease (AD), marked by cognitive impairment, predominantly affects the brain regions regulated by cholinergic innervation, such as the cerebral cortex and hippocampus. Cholinergic dysfunction, a key contributor to age-related cognitive decline, has spurred investigations into potential therapeutic interventions. We have previously shown that choline alphoscerate (α -GPC), a cholinergic neurotransmission-enhancing agent, protects from A β -mediated neurotoxicity. Herein, we investigated the effects of α -GPC on the microglial phenotype in response to A β via modulation of the nicotinic alpha-7 acetylcholine receptor ($\alpha 7$ nAChR). BV2 microglial cells were pre-treated for 1 h with α -GPC and were treated for 24, 48, and 72 h with A β_{1-42} and/or α -BTX, a selective $\alpha 7$ nAChR antagonist. Fluorescent immunocytochemistry and Western blot analysis showed that α -GPC was able to antagonize A β -induced inflammatory effects. Of note, α -GPC exerted its anti-inflammatory effect by directly activating the $\alpha 7$ nAChR receptor, as suggested by the induction of an increase in [Ca²⁺]_i and Ach-like currents. Considering that cholinergic transmission appears crucial in regulating the inflammatory profiles of glial cells, its modulation emerges as a potential pharmaco-therapeutic target to improve outcomes in inflammatory neurodegenerative disorders, such as AD.

Keywords: acetylcholine; cholinergic transmission; microglia; inflammatory response



Citation: Cantone, A.F.; Burgaletto, C.; Di Benedetto, G.; Pannaccione, A.; Secondo, A.; Bellanca, C.M.; Augello, E.; Munafò, A.; Tarro, P.; Bernardini, R.; et al. Taming Microglia in Alzheimer's Disease: Exploring Potential Implications of Choline Alphoscerate via $\alpha 7$ nAChR Modulation. *Cells* **2024**, *13*, 309. <https://doi.org/10.3390/cells13040309>

Academic Editors: John W. Chen and Michael Breckwoldt

Received: 4 January 2024

Revised: 25 January 2024

Accepted: 3 February 2024

Published: 7 February 2024



Copyright: © 2024 by the authors. Licensee MDPI, Basel, Switzerland. This article is an open access article distributed under the terms and conditions of the Creative Commons Attribution (CC BY) license (<https://creativecommons.org/licenses/by/4.0/>).

1. Introduction

Alzheimer's disease (AD) represents the most common age-related neurodegenerative disorder associated with memory deficits and cognitive decline [1]. Critical brain regions for the maintenance of cognitive processes include the cerebral cortex and hippocampus, whose cholinergic innervations are mainly provided by the basal forebrain cholinergic nuclei (BFCN) [2,3]. The dysfunction of cholinergic neurotransmission driven by the selective degeneration of BFCN has led to the formulation of the "cholinergic hypothesis of age-related cognitive dysfunction" [4]. Recognition of the pivotal role of altered cholinergic transmission in disease pathophysiology has spurred the development of therapeutic strategies aimed at restoring cholinergic function.

Cholinergic precursors represent the first potential approach aimed to counteract the cholinergic dysfunction and cognitive decline that occur in various forms of dementia [5].

Among them, choline alphoscerate (L-alpha-glycerylphosphocholine; α -GPC), given its high choline content (41% choline by weight) and ability to cross the blood–brain barrier, is one of the most used sources of choline [6]. Indeed, it has been found to be effective in improving the synthesis and release of acetylcholine [5].

The activation of nicotinic acetylcholine receptors (nAChRs) by acetylcholine in the frontal cortex of the brain has been shown to be essential for functions such as attention and working memory [7,8]. Specifically, the nicotinic alpha-7 acetylcholine receptor (α 7 nAChR), a ligand-activated ion channel, has been demonstrated to play an important role in AD [9]. Indeed, in addition to regulating neuronal plasticity and turnover, α 7 nAChR also has vital functions in microglia [10].

Microglial cells are the primary effectors of the innate immune system within the brain [11,12]. Upon activation, microglia can display a broad spectrum of phenotypes, ranging from the classical pro-inflammatory phenotype M1 to the alternative anti-inflammatory phenotype M2 [13], with α 7 nAChR playing a crucial role in mediating the above-mentioned contexts [14].

Considering the potential beneficial role of cholinergic precursors at the crossroads between neurodegeneration and neuroinflammation, in the present study, we attempted to investigate the mechanism underlying such effects using an in vitro model of AD.

Specifically, we investigated the effects of α -GPC, used as an indirect agonist of α 7 nAChR, on A β -induced microglial phenotypic switching in the BV2 murine microglial cell line. In addition, we used a selective α 7 nAChR antagonist, α -bungarotoxin, to substantiate the receptor's direct involvement in mediating this mechanism.

2. Materials and Methods

2.1. Drugs and Chemicals

All media were obtained from Thermo Fisher Scientific, Inc., Waltham, MA, USA. L-alpha-glycerylphosphocholine (α -GPC) was provided by Italfarmaco, Milano, Italy. Lyophilised amyloid- β protein fragment 1–42 was obtained from Sigma-Aldrich, St. Louis, MO, USA. All other chemicals were of the highest commercial grade.

2.2. Preparation of A β _{1–42} Oligomers

A β _{1–42} oligomers were prepared as previously described [15]. Briefly, lyophilized A β _{1–42} peptide was first dissolved in 1,1,1,3,3,3-hexafluoro-2-propanol (HFIP; Sigma-Aldrich) under a fume hood to a final concentration of 1 mM. The solution was aliquoted and incubated at room temperature (RT) for 2 h to allow monomerization. A SpeedVac centrifuge (800 \times g, RT) was used to remove traces of HFIP, and the clear peptide film was stored over desiccant at -80 °C. For oligomerization, the aliquoted peptide film was dissolved in dimethyl sulfoxide (DMSO) to 5 mM. To obtain the oligomeric form of A β _{1–42}, the peptide in DMSO was diluted directly into sterile phosphate-buffered saline (PBS, 1 \times) at 100 μ M and incubated at 4 °C for 12 h. After incubation, the A β _{1–42} samples were either used immediately for treating cells or were aliquoted and stored at -20 °C until use.

2.3. Cell Cultures

The BV2 murine microglial cell line was obtained from AcceGen (AcceGen Biotech, Fairfield, NJ, USA; Cat. ABC-TC212S; Accession Number: CVCL_0182). The cells were cultured in Dulbecco's Modified Eagle Medium (DMEM; High Glucose) supplemented with 10% (*v/v*) fetal bovine serum, 100 g/mL penicillin, 100 g/mL streptomycin, 1% (*v/v*) sodium pyruvate, and 2 mM glutamine. The cells were maintained in an atmosphere of 5% CO₂ and 95% humidified air at 37 °C.

2.4. Cell Viability Test

Cell viability was determined using a 3-[4,5 dimethylthiazol-2-yl]-2,5-diphenyltetrazolium bromide (MTT) assay. A total of 5×10^3 cells per well were plated on 96-well plates. The culture medium was changed to a medium containing MTT (Sigma-Aldrich, Milan,

Italy), and cell viability was quantified by measuring the reduction of the MTT solution (0.5 mg/mL). Following incubation for 3 h at 37 °C, the solution was removed, and dimethyl sulfoxide (DMSO) was added for cell lysis and solubilization of the blue formazan crystals resulting from MTT reduction by the mitochondrial activity of viable cells. A VarioskanTM Flash Multimode Reader was used to measure the optical density of the supernatants at 545 nm. The data were expressed as the mean percentage of viable cells compared to the control. The experiments were performed in triplicate at least twice.

2.5. Western Blot Analysis

For protein extraction and Western blot analysis, the cells were lysed in buffer containing 150 mM NaCl, 5 mM EDTA, 50 mM Tris-HCl (pH 7.5), 1 mM Na₃VO₄, 1 mM acid phenyl-methyl-sulphonyl-fluoride, 30 mM sodium pyrophosphate, 50 mM NaF, 5 µg/mL aprotinin, 2 µg/mL leupeptin, 1 µg/mL pepstatin, 10% glycerol, and 0.2% TritonTM X-100. The homogenates were then centrifuged at 14,000 rpm for 10 min at 4 °C. The protein concentration of the supernatant was determined using the Bradford method [16]. Equal amounts of protein (30 µg) were resolved on 8–12% SDS-PAGE gels and transferred onto Hybond ECL nitrocellulose membranes (GE Healthcare, Little Chalfont, UK). The membranes were blocked for 1 h at RT with 5% non-fat dry milk plus 0.05% Tween 20. For the primary antibody reactions, a rabbit anti-IL-10 antibody (Abbtotec, San Diego, CA, USA, 250713; 1:250), a rabbit anti-TNF-α antibody (Novus Biologicals, Littleton, CO, USA, NB600-587; 1:1000), or rabbit anti-α7 nAChR (Abcam, Cambridge, UK, ab216485; 1:250) were added to the membranes and incubated overnight at 4 °C on an orbital shaker. Then, the membranes were washed with PBS plus 0.05% Tween 20 (PBS-T) and were probed with the appropriate horseradish peroxidase-conjugated secondary antibody (Amersham Life Science, Buckinghamshire, UK) for 1 h at RT. β-actin (Santa Cruz Biotechnology Inc., Santa Cruz, CA, USA, sc-47778; 1:500) was used as a control to validate the amount of protein loaded in the gels. After washing three times with PBS-T, detection was performed using an ECL chemiluminescence assay (Amersham Life Science). The protein bands were scanned with the iBright FL1500 Imaging System (Thermo Fisher Scientific). The densitometric analysis of band intensity was conducted on immunoblots using IMAGE J software version 1.53v (<https://imagej.nih.gov/ij/>, accessed on 9 October 2023).

2.6. Fluorescent Immunocytochemistry

After treatment, the BV2 cells were fixed for 15 min in 4% paraformaldehyde, permeabilized for 7 min with 0.1% Triton X-100, and then blocked for 30 min with 1% BSA. The cells were incubated for 1 h at RT with mouse anti-CD86 (Santa Cruz Biotechnology Inc., Santa Cruz, CA, USA, sc-28347, 1:250), mouse anti-CD68 (Santa Cruz Biotechnology Inc., sc-20060; 1:250), a rabbit anti-IL-10 antibody (Abbtotec, 250713; 1:200), a rabbit anti-TNF-α antibody (Novus Biologicals, NB600-587; 1:100), or a rabbit anti-α7 nAChR (Abcam, ab216485; 1:500). After washing in PBS three times for 5 min each, the cells were incubated for 1 h at RT in the dark with the appropriate fluorescent-labelled secondary antibodies (Alexa Fluor 488 donkey anti-mouse (Thermo Fisher Scientific), Alexa Fluor 546 donkey anti-rabbit (Thermo Fisher Scientific), or Alexa Fluor 488 donkey anti-rabbit (Thermo Fisher Scientific)). Finally, for nuclear staining and the stabilization of fluorescent signals, the slides were covered in mounting medium (Fluoroshield with DAPI; Sigma-Aldrich, Milan, Italy) and secured with a coverslip. Fluorescence images were captured using a Zeiss Observer.Z1 microscope equipped with the Apotome.2 acquisition system (Zeiss LSM 700, Jena, Germany).

2.7. [Ca²⁺]_i Measurements

[Ca²⁺]_i was measured using single-cell Fura-2 acetoxymethyl-ester (AM) video imaging, as previously described [17]. The BV2 cells, placed on glass coverslips, were loaded with 10 µmol/L Fura-2AM for 30 min at 37 °C in normal Krebs solution containing 5.5 mM KCl, 160 mM NaCl, 1.2 mM MgCl₂, 1.5 mM CaCl₂, 10 mM glucose, and 10 mM HEPES-

NaOH (pH 7.4). $[Ca^{2+}]_i$ was measured using a live-imaging system composed of an inverted Zeiss Axiovert 200 microscope (Carl Zeiss, Goettingen, Germany), a MicroMax 512BFT cooled CCD camera (Princeton Instruments, Trenton, NJ, USA), a LAMBDA10-2 filter wheel (Sutter Instruments, Novato, CA, USA), and Meta-Morph/MetaFluor Imaging System software version 7.8 (Universal Imaging, West Chester, PA, USA). After loading, the samples were alternatively illuminated at 340 nm and 380 nm wavelengths. The drug effect on $[Ca^{2+}]_i$ was evaluated as $\Delta\%$ peak increase over basal values in the absence or presence of α -bungarotoxin. The BV2 cells were treated with the toxin for 5 min before the registration and were then analyzed.

2.8. Patch-Clamp Electrophysiology

The $\alpha 7$ nAChR currents were recorded from the BV2 cells using the patch-clamp technique in a whole-cell configuration using a commercially available amplifier (Axopatch200B (Molecular Devices, San Jose, CA, USA)), and the data were acquired using a Digidata1322A acquisition system (Molecular Devices) and pCLAMP software, version 10.5 (Molecular Devices, Burlingame, CA, USA). The peak current amplitude and charge movement (area under curve, AUC) induced by agonist application were measured using ClampFit 10 (Molecular Devices). The borosilicate microelectrode (resistance of 4–5 M Ω) was prepared with a puller (Narishige, PC-10, Tokyo, Japan). The dialyzing pipette solution contained the following (in mM): 100 Cs-gluconate, 10 TEA, 20 NaCl, 1 Mg-ATP, 0.1 CaCl₂, 2 MgCl₂, 0.75 EGTA, and 10 HEPES, adjusted to a pH of 7.2 using CsOH. The cells were perfused with external Ringer's solution containing the following (in mM): 126 NaCl, 1.2 NaHPO₄, 2.4 KCl, 2.4 CaCl₂, 1.2 MgCl₂, 10 glucose, and 18 NaHCO₃, with a pH of 7.4. The holding potential was maintained at -70 mV to record the Ach currents. The currents were filtered at 2 kHz and digitized at 10 kHz. The drugs were applied using a hand-held pipette at the following concentrations: 1 mM acetylcholine, 1 mM α -GPC, and 10 nM α -bungarotoxin.

2.9. Statistical Evaluation

All the experiments were run in triplicate. The data were analyzed using the one-way ANOVA test, followed by the Bonferroni post-hoc test. Statistical evaluation was performed using standard computer software (SPSS software package, ver. 23.0, SPSS Inc., Chicago, IL, USA). Statistical significance was set at a $p < 0.05$. The graph design and statistical analyses were performed using Graph Pad Prism (Ver. 8, La Jolla, CA, USA).

3. Results

3.1. Alpha-GPC Counteracts A β -Induced Toxicity in BV2 Microglial Cells

To assess α -GPC's potential protective role on BV2 microglial cells against A β toxicity, viability experiments were conducted using the MTT assay. Initially, we tested the concentration-related effect (ranging from 1 pM to 100 μ M) of α -GPC alone on BV2 microglial cell viability following treatment for 24, 48, and 72 h. α -GPC did not significantly affect cell proliferation, nor did it induce cell toxicity at low concentrations. Nevertheless, at concentrations of 25, 50, and 100 μ M, α -GPC showed toxic effects, as demonstrated by a significant decrease in cell viability at all the time points studied.

Consistent with these observations, α -GPC at 1 μ M was chosen for the subsequent experiments. To explore whether α -GPC exerts a protective effect against A β -related toxicity on BV2 cells, the cells were pre-treated for 1 h with α -GPC 1 μ M and were treated for 24, 48, and 72 h with α -GPC 1 μ M and/or A β_{1-42} (5 μ M). α -GPC was able to mitigate the A β_{1-42} -induced detrimental effect on BV2 microglial cells at all the time points studied (Figure 1).

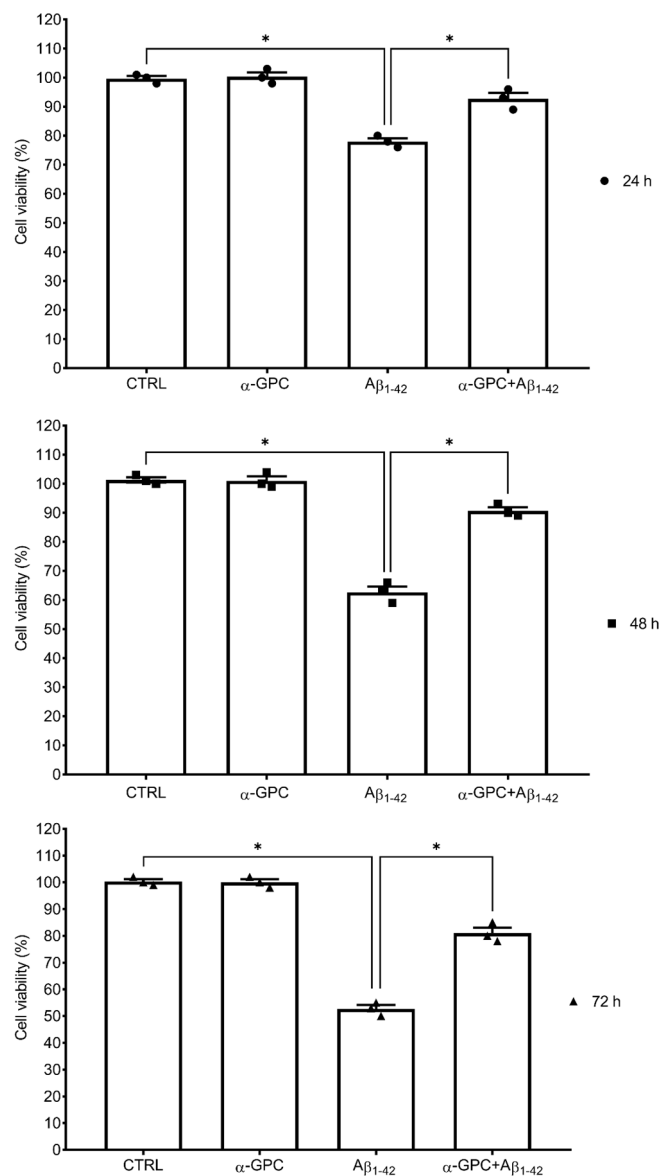


Figure 1. α -GPC mitigates the $A\beta_{1-42}$ -induced detrimental effect on BV2 microglial cells. The cell viability (%) of BV2 microglial cells pre-treated for 1 h with α -GPC (1 μ M) and treated for 24, 48, or 72 h with $A\beta_{1-42}$ (5 μ M). The vertical bars represent the means \pm S.E.M. One-way ANOVA and the Bonferroni post-hoc test were used for statistical analysis. * $p < 0.05$.

3.2. α -GPC Blunts the $A\beta$ -Induced Inflammatory Phenotype in BV2 Microglial Cells

To investigate whether the protective effect of α -GPC on BV2 microglia exposed to $A\beta$ was also associated with changes in microglia phenotype, the expression of phenotype-associated molecules was analyzed by means of immunofluorescence analysis. The BV2 cells were treated with $A\beta_{1-42}$ (5 μ M) for 48 h, either alone or in combination with α -GPC 1 μ M (1 h of pre-treatment and treatment for 48 h). The time point of 48 h was selected for the subsequent experiments, as it represents the time point at which the microglial inflammatory phenotypes were activated [18].

As shown in Figure 2, $A\beta$ treatment significantly increased the expression of CD86 and TNF- α in BV2 cells, indicative of the M1 pro-inflammatory phenotype. In contrast, α -GPC treatment prior to $A\beta$ stimulation significantly counteracted the $A\beta$ -induced increase of CD86 and TNF- α (Figure 2).

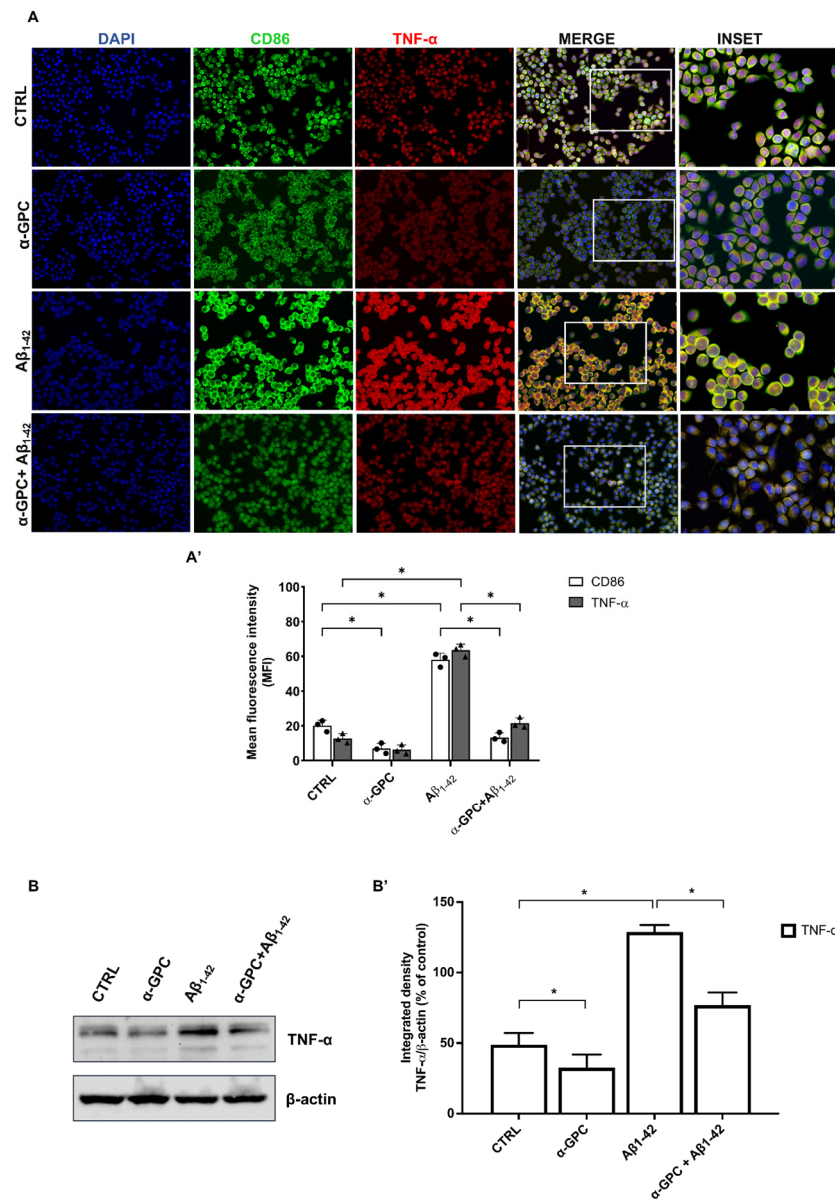


Figure 2. Pro-inflammatory microglia were blunted by α -GPC treatment. (A) Representative images (original magnification 20 \times ; inset 40 \times) of the fluorescent immunocytochemical detection of CD86 and TNF- α expression in BV2 cells pre-treated for 1 h with α -GPC (1 μ M) and treated for 48 h with A β ₁₋₄₂ (5 μ M) and the respective mean fluorescence intensity (MFI) analysis (A'), the boxes in the fourth column represent the selected magnified area shown in the fifth column (inset). (B) Western blot for TNF- α protein expression in BV2 cells and the respective densitometric analysis (B'). The data are expressed as means \pm S.E.M. One-way ANOVA and the Bonferroni post-hoc test were used to determine statistical significance. * $p < 0.05$.

Consistently, A β treatment decreased the expression of the anti-inflammatory markers CD68 and IL-10, whereas pre-treatment with α -GPC was able to increase their expression in the BV2 cells that underwent A β treatment (Figure 3). The Western blot analysis (Figure 2) further confirmed that the expression of TNF- α was substantially increased in BV2 cells challenged with A β ₁₋₄₂, whereas pre-treatment with α -GPC significantly attenuated its expression. On the other hand, the expression of IL-10 was reduced in BV2 cells challenged with A β ₁₋₄₂ and was significantly increased by pre-treatment with α -GPC (Figure 3).

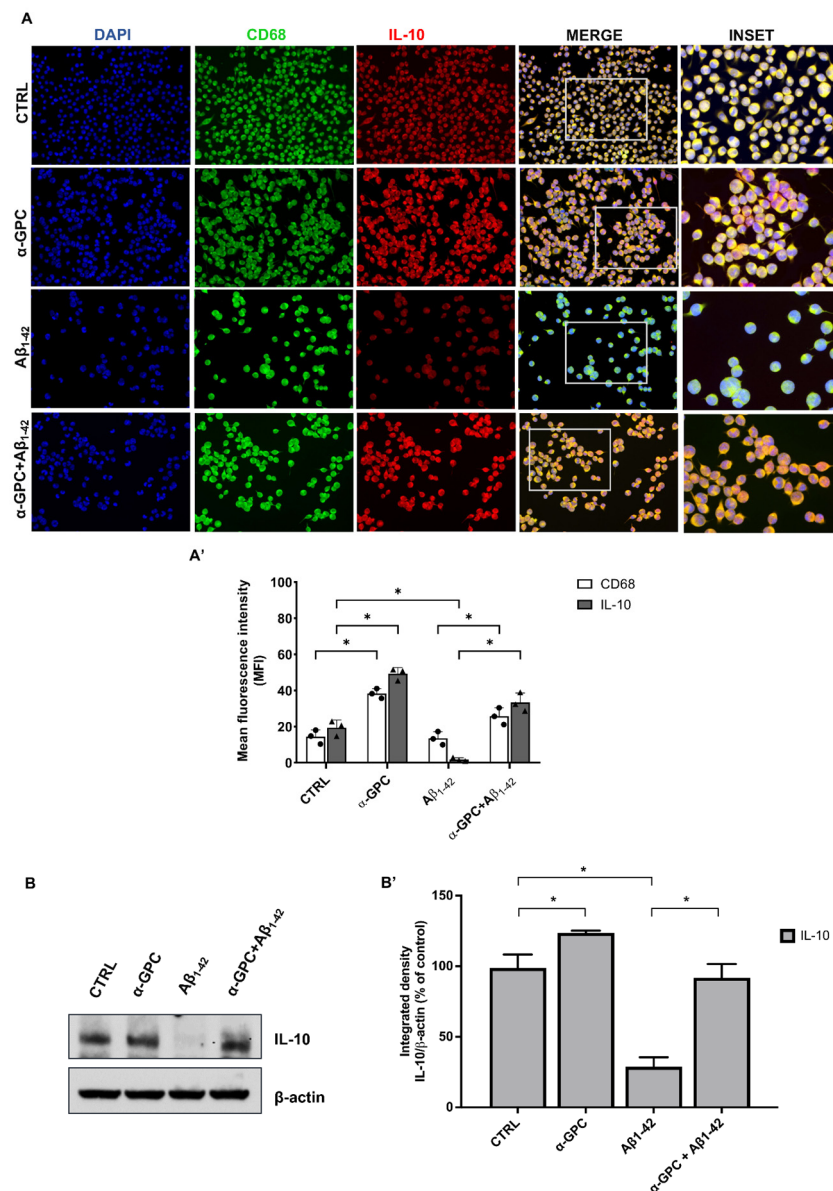


Figure 3. α -GPC contributes to the switching of microglia toward a pro-inflammatory phenotype. (A) Representative images (original magnification 20 \times ; inset 40 \times) of the fluorescent immunocytochemical detection of CD68 and IL-10 expression in BV2 cells pre-treated for 1 h with α -GPC (1 μ M) and treated for 48 h with A β ₁₋₄₂ (5 μ M) and the respective mean fluorescence intensity (MFI) analysis (A'), the boxes in the fourth column represent the selected magnified area shown in the fifth column (inset). (B) Western blot for IL-10 protein expression in BV2 cells and the respective densitometric analysis (B'). The data are expressed as means \pm S.E.M. One-way ANOVA and the Bonferroni post-hoc test were used to determine statistical significance. * $p < 0.05$.

In addition to the previously highlighted positive effects of α -GPC on BV2 cells subjected to A β treatment, it is noteworthy that α -GPC alone was able to regulate the protein expression of TNF- α and IL-10 compared to the control group (Figures 2 and 3).

3.3. α -GPC Treatment Modulates $\alpha 7$ nAChR Expression in BV2 Cells

The expression of $\alpha 7$ nAChR in BV2 microglial cells is well-documented [19], and it is established that the activation of microglial $\alpha 7$ nAChR suppresses the production of several pro-inflammatory molecules [20]. To investigate the potential impact of α -GPC treatment on $\alpha 7$ nAChR expression in microglia exposed to A β , we performed fluorescent

immunocytochemistry in BV2 cells challenged with $A\beta_{1-42}$ (5 μ M) for 48 h, either alone or after a 1 h pre-treatment with α -GPC (1 μ M).

Although BV2 cell cultures challenged with $A\beta$ showed reduced expression of $\alpha 7$ nAChR compared to untreated cells, pre-treatment with α -GPC increased its expression (Figure 4).

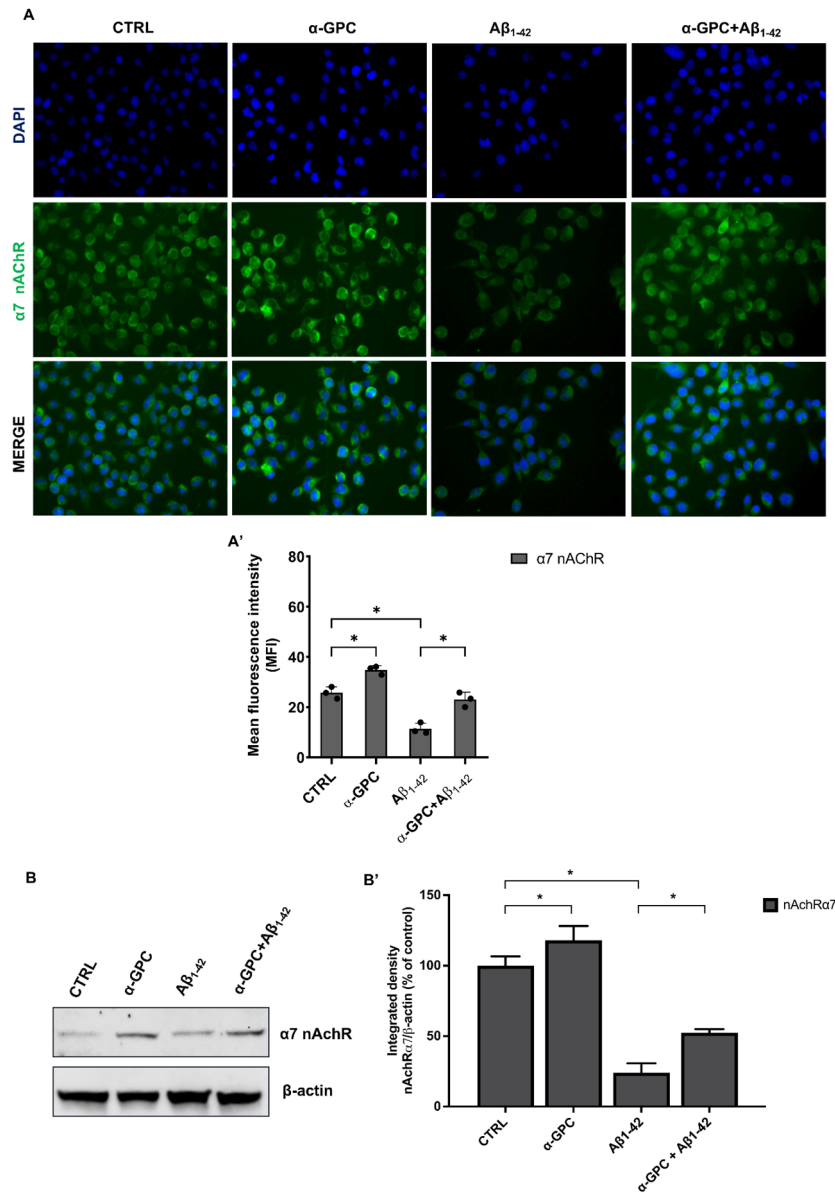


Figure 4. $\alpha 7$ nAChR is modulated by α -GPC treatment. (A) The fluorescent immunocytochemistry detection (original magnification 20 \times) of $\alpha 7$ nAChR in BV2 cells pre-treated with α -GPC (1 μ M) and treated for 48 h with $A\beta_{1-42}$ (5 μ M) and the respective mean fluorescence intensity (MFI) analysis (A'). (B) Western blot for $\alpha 7$ nAChR protein expression in BV2 cells and the respective densitometric analysis (B'). The data are expressed as means \pm S.E.M. One-way ANOVA and the Bonferroni post-hoc test were used to determine statistical significance. * $p < 0.05$.

Consistent with these findings, the Western blot analysis of lysates of BV2 cells treated with α -GPC and/or $A\beta_{1-42}$, conducted to verify the modulation of $\alpha 7$ nAChR expression, corroborated previous data (Figure 4). In addition to the positive effects of α -GPC on $A\beta$ -treated BV2 cells, it is worth noting that α -GPC increased $\alpha 7$ nAChR protein expression compared to the control group.

3.4. Alpha-Bungarotoxin Prevents the Effect of α -GPC on α 7-nAChR-Mediated $[Ca^{2+}]_i$ Increase and Inward Currents in Microglial Cells

To investigate whether the beneficial effects of α -GPC on microglia are mediated by the α 7 nAChR, the BV2 cells were challenged with α -GPC or acetylcholine (ACh) alone and in combination with α -BTX, an antagonist of α 7 nAChR, to measure the $[Ca^{2+}]_i$ and ACh currents.

The results showed that ACh induced a significant increase in $[Ca^{2+}]_i$ in Fura2-loaded BV2 cells and a rapid inward current measured using patch-clamp electrophysiology, effects that were inhibited by treatment with α -BTX (Figure 5).

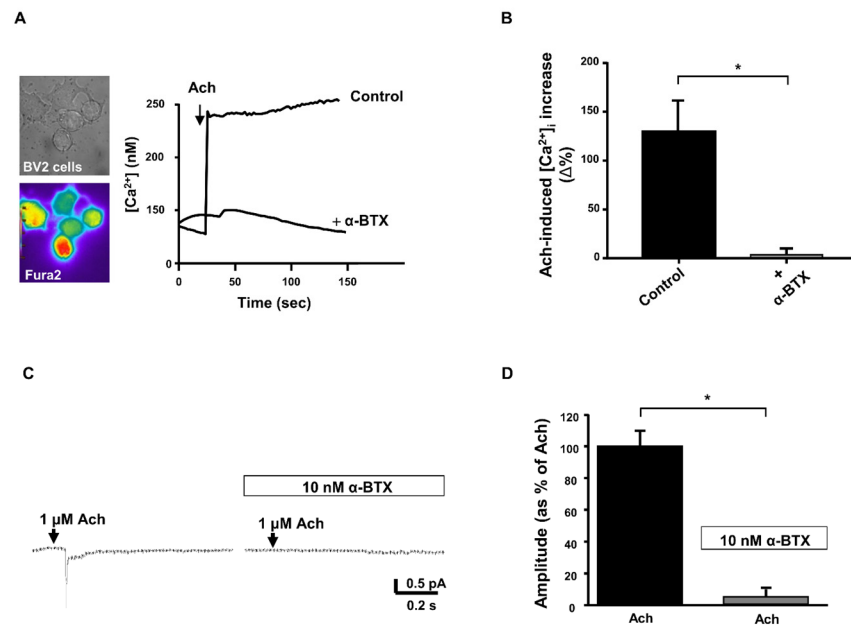


Figure 5. Effect of α -bungarotoxin on acetylcholine-induced $[Ca^{2+}]_i$ increase and acetylcholine-induced inward current in microglial BV2 cells. (A) Representative traces and quantification (B) for the effect of acetylcholine (ACh, $1 \mu\text{M}$) alone or in the presence of α -bungarotoxin (10 nM) on $[Ca^{2+}]_i$, expressed as the $\Delta\%$ increase peak over basal values ($N = 40$ cells for ACh and $N = 35$ cells for ACh + α -BTX). On the left, the representative brightfield and pseudocolor images of Fura-2 loaded BV2 cells are shown. (C) Representative current traces in response to ACh ($1 \mu\text{M}$) alone or in the presence of α -BTX (10 nM), and the quantification of current amplitude (D). The values are expressed as the mean \pm SEM of three independent experimental sessions ($N = 8$ cells for ACh and $N = 10$ cells for ACh + α -BTX). * $p < 0.05$.

Interestingly, α -GPC was able to significantly increase the $[Ca^{2+}]_i$ in a concentration-dependent manner (Figure 6A), with the highest observed increase at the concentration of $1 \mu\text{M}$. Moreover, α -BTX prevented the α -GPC-induced effect on $[Ca^{2+}]_i$ (Figure 6B), suggesting its ability to selectively modulate the α 7 nAChR receptor in microglial cells. Indeed, α -GPC elicited an inward current that was found to be higher than that elicited by ACh, and this effect was blocked by α -BTX, as demonstrated by the patch-clamp-detected current amplitude (Figure 6C,D). Accordingly, the observed current was the result of delayed current inactivation (Figure 6E).

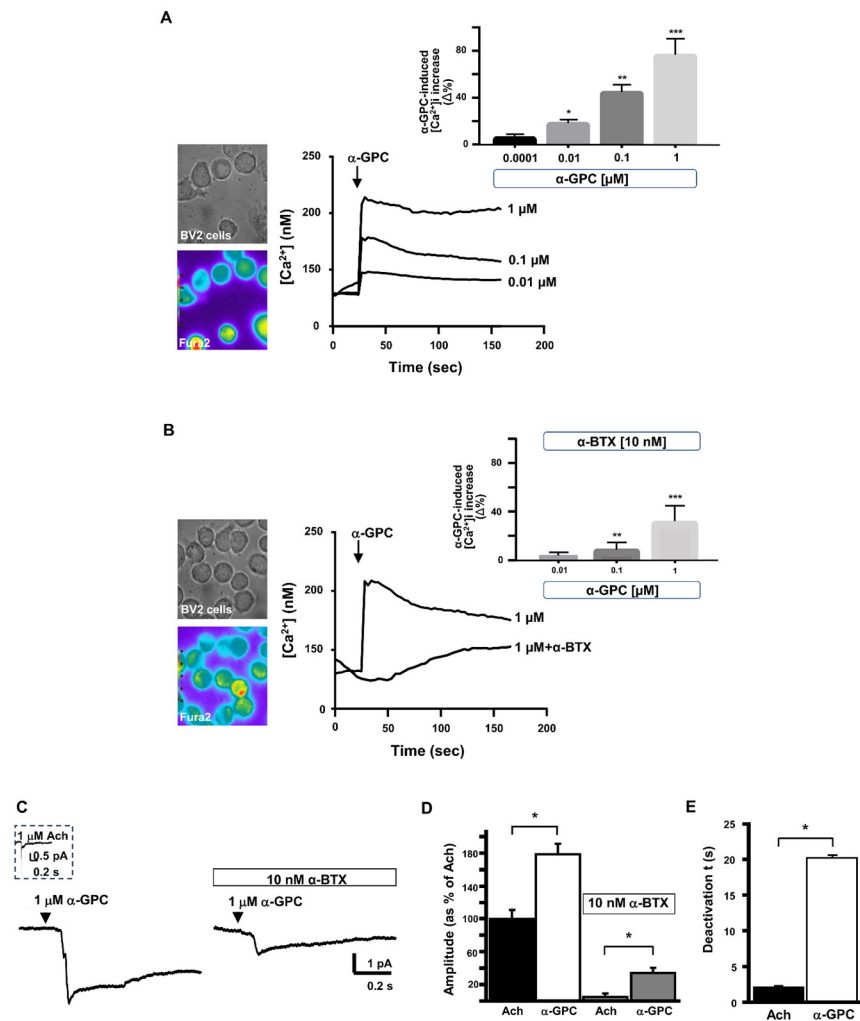


Figure 6. Effect of α -GPC on $[Ca^{2+}]_i$ increase and the $\alpha 7$ -nAChR-encoded inward current in microglial BV2 cells. (A) Representative traces and quantification (B) for the effect of different concentrations of α -GPC (0.01–1 μ M) alone or α -GPC (1 μ M) + α -BTX (10 nM) on $[Ca^{2+}]_i$, expressed as the $\Delta\%$ increase peak over basal values ($N = 35$ cells for α -GPC and $N = 30$ cells for α -GPC + α -BTX). On the left of each panel, the representative brightfield and pseudocolor images of Fura-2 loaded BV2 cells are shown. * $p < 0.05$ vs. control (basal values) and 0.0001 μ M; ** $p < 0.05$ vs. control and 0.01 μ M; *** $p < 0.05$ vs. all. (C) Representative traces of Ach-like currents elicited by α -GPC (1 μ M) alone or + α -BTX (10 nM), and the quantification of current amplitude (D). The values are expressed as the mean \pm SEM of three independent experimental sessions ($N = 9$ cells for α -GPC and $N = 12$ cells for α -GPC + α -BTX). (E) Quantification of the slow deactivation induced by α -GPC. * $p < 0.05$.

3.5. Alpha-Bungarotoxin Reverts the Effects of α -GPC on Anti-Inflammatory Signaling Molecules

To assess the role of $\alpha 7$ nAChR in the regulation of the anti-inflammatory effects mediated by α -GPC, we performed experiments on BV2 cells challenged with α -BTX, either alone or in the presence of α -GPC and/or $A\beta_{1-42}$. The expression of pro-inflammatory markers CD86 and TNF- α , as well as the anti-inflammatory markers CD68 and IL-10, was evaluated using fluorescence immunocytochemistry. The results showed that α -BTX was able to inhibit the anti-inflammatory effect induced by α -GPC in BV2 microglial cells challenged with $A\beta_{1-42}$, as demonstrated by the substantial increase in the expression of inflammatory markers (Figure 7).

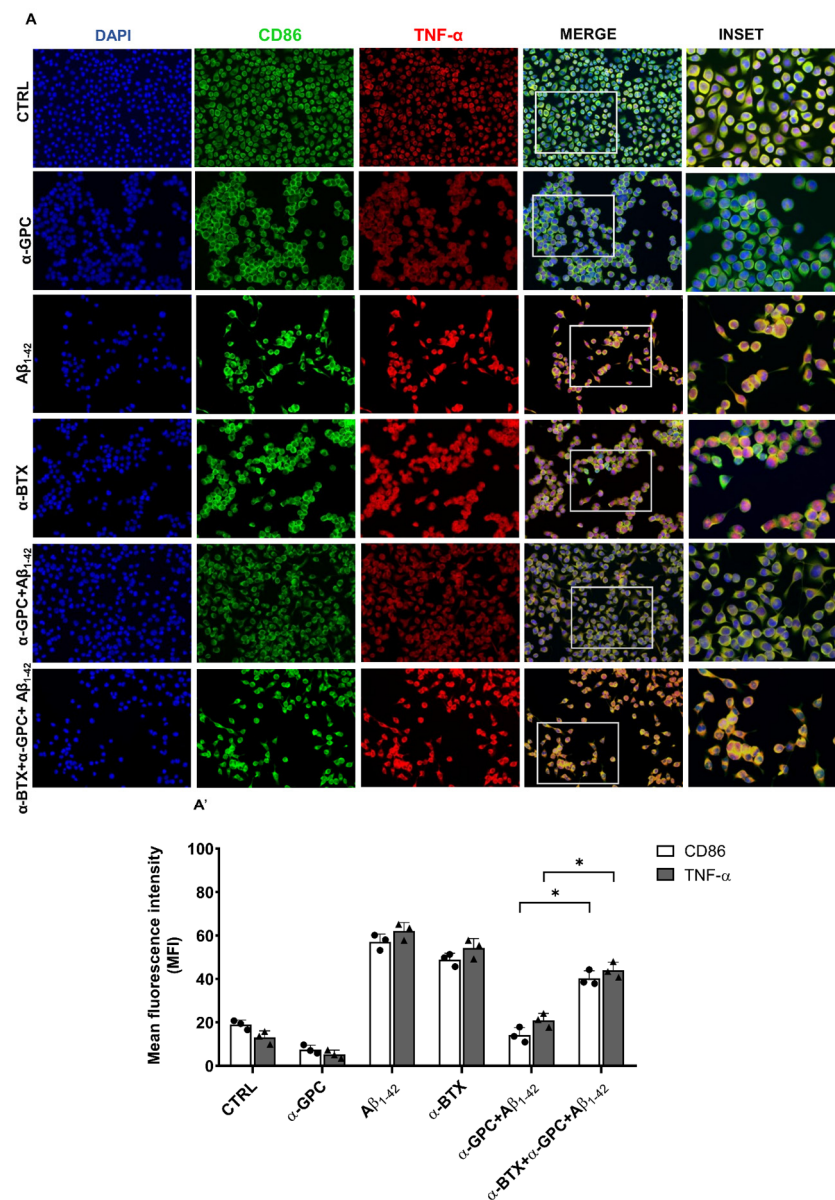


Figure 7. α -BTX restores the expression of pro-inflammatory molecules. (A) Representative images (original magnification 20 \times ; inset 40 \times) of the fluorescent immunocytochemical detection of CD86 and TNF- α expression in BV2 cells pre-treated for 1 h with α -GPC (1 μ M) and treated for 48 h with A β ₁₋₄₂ (5 μ M)/ α -BTX (100 nM) and the respective mean fluorescence intensity (MFI) analysis (A'), the boxes in the fourth column represent the selected magnified area shown in the fifth column (inset). The data are expressed as means \pm S.E.M. Differences between the groups were considered significant at * $p < 0.05$ (One-way ANOVA followed by the Bonferroni post-hoc test).

On the other hand, α -BTX treatment blunted the expression of both IL-10 and CD68 in BV2 microglial cells pre-treated with α -GPC and challenged with A β ₁₋₄₂ (Figure 8).

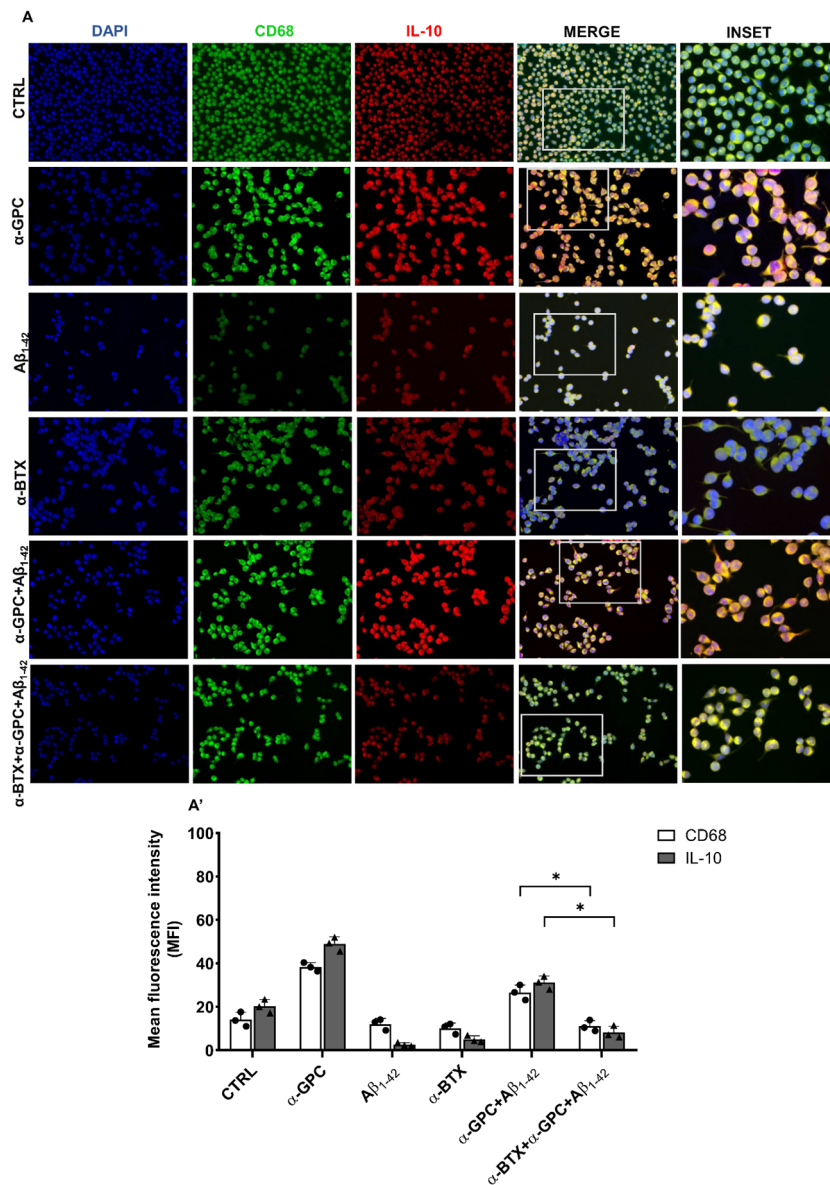


Figure 8. α -BTX inhibits the anti-inflammatory effects of α -GPC. (A) Representative images (original magnification 20 \times ; inset 40 \times) of the fluorescent immunocytochemical detection of CD68 and IL-10 expression in BV2 cells pre-treated for 1 h with α -GPC (1 μ M) and treated for 48 h with A β _{1–42} (5 μ M)/ α -BTX (100 nM) and the respective mean fluorescence intensity (MFI) analysis (A'), the boxes in the fourth column represent the selected magnified area shown in the fifth column (inset). The data are expressed as means \pm S.E.M. Differences between the groups were considered significant at * $p < 0.05$ (One-way ANOVA followed by the Bonferroni post-hoc test).

4. Discussion

In the evolving landscape of AD therapeutics, characterized by treatments that primarily address symptoms with limited disease-modifying properties [21], our study explored the potential of choline alphoscerate (α -GPC).

Despite being available in the pharmaceutical market since 1987, the interest in α -GPC declined after the introduction of cholinesterase inhibitors. However, over the past decade, renewed attention has been given to this choline-containing phospholipid in several pre-clinical studies and clinical investigations [5,22,23].

In the present study, we investigated the effects of α -GPC, used as an indirect agonist of $\alpha 7$ nAChR, in an in vitro model of microglia in AD. The primary objective was to elucidate whether α -GPC holds dual protective capacity, not only safeguarding neuronal

cells from A β -induced toxicity [24,25] but also orchestrating a concurrent protective effect in microglial cells challenged with A β _{1–42}.

Our findings showcase that, although α -GPC did not interfere with cell survival, it effectively counteracted the detrimental effects induced by A β _{1–42} in BV2 microglial cells.

Similar to Ach, α -GPC, which contains choline in its structure and may act as a precursor to Ach, can modulate microglial activity in response to A β , involving changes in cytokines release, phagocytic activity, and other microglial functions [26].

Our observations unveiled a remarkable aspect of α -GPC as it prompted a discernible transition in A β -activated microglia from the pro-inflammatory M1 phenotype to the protective M2 phenotype. Specifically, when BV2 microglial cells were exposed to A β _{1–42}, they manifested a heightened pro-inflammatory state typical of the M1 phenotype, characterized by the high expression of CD86 and TNF- α . TNF- α , primarily produced by microglia, astrocytes, and neurons in response to various stimuli [27], represents a key molecule in orchestrating chronic inflammation. Indeed, TNF- α can have an impact on A β plaque synthesis and neurofibrillary tangle formation, fueling the progression of AD pathology [28,29].

Of note, α -GPC treatment in the presence of A β _{1–42} induced a distinct phenotypic shift towards the M2 status, characterized by a significant attenuation of the expression of inflammatory markers and a concurrent increase in the anti-inflammatory cytokine IL-10, a cytokine known to act on amyloid and reduce pro-inflammatory molecules [30].

Several studies indicate the presence of a parasympathetic mechanism that suppresses the release of inflammatory cytokines, thereby regulating inflammation. This mechanism, known as the “cholinergic anti-inflammatory pathway”, shows that acetylcholine inhibits the release of pro-inflammatory cytokines, such as TNF- α , IL-6, and IL-1 β , in primary human macrophages [31]. Studies conducted using antisense oligonucleotides of the α 7 subunit revealed α 7 nAChR as the main player of the above-mentioned process [32], shedding light on its role in orchestrating the choline-mediated anti-inflammatory effects [33–36]. Indeed, it has been reported that α 7 nAChRs expressed by glial cells may counterbalance the neuroinflammatory effects of A β fragments [37]. The activation of α 7 nAChRs with a selective agonist has been reported to promote A β phagocytosis by cultured microglial cells [37] and improve cognitive function in an AD mouse model [38].

It is well established that among nicotinic receptors, the homomeric α 7 subtype exhibits one of the highest Ca²⁺: Na⁺ permeability ratios [39]. Considering the multitude of cellular pathways regulated by calcium influx through this receptor, particularly those associated with neuroprotection [40,41], we measured [Ca²⁺]_i.

Delving into the specific role of α 7 nAChR, known for its involvement in cognition [42], attention [43], and neuroprotection [44], we investigated the functional dynamics of α 7 nAChR in BV2 microglia in response to α -GPC or acetylcholine (Ach), used as an endogenous agonist, either in the presence or absence of the α 7-nAChR-specific inhibitor α -bungarotoxin (α -BTX).

Interestingly, we observed that α -GPC, resembling the actions of Ach, induced a rapid inward current that was found to be higher than that elicited by the endogenous agonist Ach in BV2 microglia, and this dynamic effect was almost entirely blocked by the α 7 inhibitor α -bungarotoxin (α -BTX). These observations further support the ability of α -GPC to selectively modulate the α 7 nAChR receptors in microglial cells.

In line with this, our results suggest that the choline-mediated anti-inflammatory effects are mediated by α 7 nicotinic receptors and reversed by the selective α 7 nicotinic receptor antagonist α -BTX [45].

5. Conclusions

In conclusion, our study suggests that α -GPC may play a significant role in counteracting inflammation associated with AD. This potential anti-inflammatory effect may be attributed to its ability to enhance cholinergic stimuli and activate the α 7 nicotinic acetylcholine receptor system. Although further studies are needed to confirm its therapeutic use,

α -GPC represents a promising strategy to mitigate neuroinflammation and AD pathology, considering its non-invasiveness and clinical tolerability [46].

Author Contributions: Conceptualization, G.C., C.B. and A.F.C.; methodology, A.F.C., A.P., A.S. and G.D.B.; validation, G.D.B., A.P. and A.S.; formal analysis, C.B. and A.F.C.; writing—original draft preparation, G.C., R.B. and C.B.; writing—review and editing, A.F.C., C.B., C.M.B., E.A., A.M. and P.T.; supervision, G.C. and R.B.; funding acquisition, R.B. All authors have read and agreed to the published version of the manuscript.

Funding: This research was funded by the Italian Ministry of Research (PRIN grant no. 2017YH3SXX).

Institutional Review Board Statement: Not applicable.

Informed Consent Statement: Not applicable.

Data Availability Statement: The data presented in this study are available from the corresponding author on reasonable request.

Acknowledgments: This study was supported by an unconditional contribution from Italfarmaco S.p.A., Milano, Italy.

Conflicts of Interest: The authors declare no conflicts of interest.

References

1. DeTure, M.A.; Dickson, D.W. The Neuropathological Diagnosis of Alzheimer's Disease. *Mol. Neurodegener.* **2019**, *14*, 32. [[CrossRef](#)]
2. Martinez, J.L.; Zammit, M.D.; West, N.R.; Christian, B.T.; Bhattacharyya, A. Basal Forebrain Cholinergic Neurons: Linking Down Syndrome and Alzheimer's Disease. *Front. Aging Neurosci.* **2021**, *13*, 703876. [[CrossRef](#)] [[PubMed](#)]
3. Ballinger, E.; Ananth, M.; Talmage, D.A.; Role, L. Basal Forebrain Cholinergic Circuits and Signaling in Cognition and Cognitive Decline. *Neuron* **2016**, *91*, 1199–1218. [[CrossRef](#)]
4. Hampel, H.; Mesulam, M.-M.; Cuello, A.C.; Farlow, M.R.; Giacobini, E.; Grossberg, G.T.; Khachaturian, A.S.; Vergallo, A.; Cavedo, E.; Snyder, P.J.; et al. The Cholinergic System in the Pathophysiology and Treatment of Alzheimer's Disease. *Brain* **2018**, *141*, 1917–1933. [[CrossRef](#)] [[PubMed](#)]
5. Traini, E.; Bramanti, V.; Amenta, F. Choline Alphoscerate (Alpha-Glyceryl-Phosphoryl-Choline) an Old Choline-Containing Phospholipid with a Still Interesting Profile as Cognition Enhancing Agent. *Curr. Alzheimer Res.* **2013**, *10*, 1070–1079. [[CrossRef](#)]
6. Kansakar, U.; Trimarco, V.; Mone, P.; Varzideh, F.; Lombardi, A.; Santulli, G. Choline Supplements: An Update. *Front. Endocrinol.* **2023**, *14*, 1148166. [[CrossRef](#)]
7. Hurst, R.; Rollema, H.; Bertrand, D. Nicotinic Acetylcholine Receptors: From Basic Science to Therapeutics. *Pharmacol. Ther.* **2013**, *137*, 22–54. [[CrossRef](#)] [[PubMed](#)]
8. Galvin, V.C.; Arnsten, A.F.T.; Wang, M. Involvement of Nicotinic Receptors in Working Memory Function. In *Behavioral Pharmacology of the Cholinergic System*; Shoab, M., Wallace, T.L., Eds.; Current Topics in Behavioral Neurosciences; Springer International Publishing: Cham, Switzerland, 2020; Volume 45, pp. 89–99, ISBN 978-3-030-56012-6.
9. Ma, K.-G.; Qian, Y.-H. Alpha 7 Nicotinic Acetylcholine Receptor and Its Effects on Alzheimer's Disease. *Neuropeptides* **2019**, *73*, 96–106. [[CrossRef](#)]
10. Orr-Urtreger, A.; Broide, R.S.; Kasten, M.R.; Dang, H.; Dani, J.A.; Beaudet, A.L.; Patrick, J.W. Mice Homozygous for the L250T Mutation in the A7 Nicotinic Acetylcholine Receptor Show Increased Neuronal Apoptosis and Die Within 1 Day of Birth. *J. Neurochem.* **2000**, *74*, 2154–2166. [[CrossRef](#)]
11. Yin, J.; Valin, K.L.; Dixon, M.L.; Leavenworth, J.W. The Role of Microglia and Macrophages in CNS Homeostasis, Autoimmunity, and Cancer. *J. Immunol. Res.* **2017**, *2017*, 5150678. [[CrossRef](#)]
12. Burgaletto, C.; Munafò, A.; Di Benedetto, G.; De Francisci, C.; Caraci, F.; Di Mauro, R.; Bucolo, C.; Bernardini, R.; Cantarella, G. The Immune System on the TRAIL of Alzheimer's Disease. *J. Neuroinflamm.* **2020**, *17*, 298. [[CrossRef](#)]
13. Cherry, J.D.; Olschowka, J.A.; O'Banion, M.K. Neuroinflammation and M2 Microglia: The Good, the Bad, and the Inflamed. *J. Neuroinflamm.* **2014**, *11*, 98. [[CrossRef](#)]
14. Akiyama, H.; Barger, S.; Barnum, S.; Bradt, B.; Bauer, J.; Cole, G.M.; Cooper, N.R.; Eikelenboom, P.; Emmerling, M.; Fiebich, B.L.; et al. Inflammation and Alzheimer's Disease. *Neurobiol. Aging* **2000**, *21*, 383–421. [[CrossRef](#)]
15. Fa, M.; Orozco, I.J.; Francis, Y.I.; Saeed, F.; Gong, Y.; Arancio, O. Preparation of Oligomeric Beta-Amyloid 1-42 and Induction of Synaptic Plasticity Impairment on Hippocampal Slices. *J. Vis. Exp.* **2010**, *41*, e1884. [[CrossRef](#)]
16. Bradford, M.M. A Rapid and Sensitive Method for the Quantitation of Microgram Quantities of Protein Utilizing the Principle of Protein-Dye Binding. *Anal. Biochem.* **1976**, *72*, 248–254. [[CrossRef](#)]
17. Boscia, F.; Gala, R.; Pannaccione, A.; Secondo, A.; Scorziello, A.; Di Renzo, G.; Annunziato, L. NCX1 Expression and Functional Activity Increase in Microglia Invading the Infarct Core. *Stroke* **2009**, *40*, 3608–3617. [[CrossRef](#)]
18. Pan, X.; Zhu, Y.; Lin, N.; Zhang, J.; Ye, Q.; Huang, H.; Chen, X. Microglial Phagocytosis Induced by Fibrillar β -Amyloid Is Attenuated by Oligomeric β -Amyloid: Implications for Alzheimer's Disease. *Mol. Neurodegener.* **2011**, *6*, 45. [[CrossRef](#)]

19. Nakamura, Y.; Kimura, S.; Takada, N.; Takemura, M.; Iwamoto, M.; Hisaoka-Nakashima, K.; Nakata, Y.; Morioka, N. Stimulation of Toll-like Receptor 4 Downregulates the Expression of A7 Nicotinic Acetylcholine Receptors via Histone Deacetylase in Rodent Microglia. *Neurochem. Int.* **2020**, *138*, 104751. [[CrossRef](#)]
20. Suzuki, T.; Hide, I.; Matsubara, A.; Hama, C.; Harada, K.; Miyano, K.; Andrä, M.; Matsubayashi, H.; Sakai, N.; Kohsaka, S.; et al. Microglial A7 Nicotinic Acetylcholine Receptors Drive a Phospholipase C/IP 3 Pathway and Modulate the Cell Activation toward a Neuroprotective Role. *J. Neurosci. Res.* **2006**, *83*, 1461–1470. [[CrossRef](#)] [[PubMed](#)]
21. Sheikh, M.; Khan, S.J.; Butt, H.A.T.; Zaidi, S.A.T.; Na, V. From Symptomatic Treatment to Disease Modification: A Turning Point in Alzheimer's Disease Management. *Cureus* **2023**, *15*, e47251. [[CrossRef](#)] [[PubMed](#)]
22. Roy, P.; Tomassoni, D.; Nittari, G.; Traini, E.; Amenta, F. Effects of Choline Containing Phospholipids on the Neurovascular Unit: A Review. *Front. Cell Neurosci.* **2022**, *16*, 988759. [[CrossRef](#)]
23. Sagaro, G.G.; Traini, E.; Amenta, F. Activity of Choline Alfoscerate on Adult-Onset Cognitive Dysfunctions: A Systematic Review and Meta-Analysis. *JAD* **2023**, *92*, 59–70. [[CrossRef](#)]
24. Burgalotto, C.; Di Benedetto, G.; Munafò, A.; Bernardini, R.; Cantarella, G. Beneficial Effects of Choline Alfoscerate on Amyloid- β Neurotoxicity in an In Vitro Model of Alzheimer's Disease. *CAR* **2021**, *18*, 298–309. [[CrossRef](#)]
25. Catanesi, M.; d'Angelo, M.; Antonosante, A.; Castelli, V.; Alfonsetti, M.; Benedetti, E.; Desideri, G.; Ferri, C.; Cimini, A. Neuroprotective Potential of Choline Alfoscerate against B-amyloid Injury: Involvement of Neurotrophic Signals. *Cell Biol. Int.* **2020**, *44*, 1734–1744. [[CrossRef](#)]
26. Tayebati, S.; Amenta, F.; Tomassoni, D. Cerebrovascular and Blood-Brain Barrier Morphology in Spontaneously Hypertensive Rats: Effect of Treatment with Choline Alfoscerate. *CNSDDT* **2015**, *14*, 421–429. [[CrossRef](#)]
27. Olmos, G.; Lladó, J. Tumor Necrosis Factor Alpha: A Link between Neuroinflammation and Excitotoxicity. *Mediat. Inflamm.* **2014**, *2014*, 861231. [[CrossRef](#)]
28. Zheng, C.; Zhou, X.-W.; Wang, J.-Z. The Dual Roles of Cytokines in Alzheimer's Disease: Update on Interleukins, TNF- α , TGF- β and IFN- γ . *Transl. Neurodegener.* **2016**, *5*, 7. [[CrossRef](#)]
29. Plantone, D.; Pardini, M.; Righi, D.; Manco, C.; Colombo, B.M.; De Stefano, N. The Role of TNF- α in Alzheimer's Disease: A Narrative Review. *Cells* **2023**, *13*, 54. [[CrossRef](#)] [[PubMed](#)]
30. Magalhães, C.A.; das Graças Carvalho, M.; de Sousa, L.P.; Caramelli, P.; Gomes, K.B. Alzheimer's Disease and Cytokine IL-10 Gene Polymorphisms: Is There an Association? *Arq. Neuropsiquiatr.* **2017**, *75*, 649–656. [[CrossRef](#)] [[PubMed](#)]
31. Borovikova, L.V.; Ivanova, S.; Zhang, M.; Yang, H.; Botchkina, G.I.; Watkins, L.R.; Wang, H.; Abumrad, N.; Eaton, J.W.; Tracey, K.J. Vagus Nerve Stimulation Attenuates the Systemic Inflammatory Response to Endotoxin. *Nature* **2000**, *405*, 458–462. [[CrossRef](#)] [[PubMed](#)]
32. Wang, H.; Yu, M.; Ochani, M.; Amella, C.A.; Tanovic, M.; Susarla, S.; Li, J.H.; Wang, H.; Yang, H.; Ulloa, L.; et al. Nicotinic Acetylcholine Receptor Alpha7 Subunit Is an Essential Regulator of Inflammation. *Nature* **2003**, *421*, 384–388. [[CrossRef](#)]
33. Piovesana, R.; Salazar Intriago, M.S.; Dini, L.; Tata, A.M. Cholinergic Modulation of Neuroinflammation: Focus on A7 Nicotinic Receptor. *Int. J. Mol. Sci.* **2021**, *22*, 4912. [[CrossRef](#)]
34. Gallowitsch-Puerta, M.; Tracey, K.J. Immunologic Role of the Cholinergic Anti-Inflammatory Pathway and the Nicotinic Acetylcholine A7 Receptor. *Ann. N. Y. Acad. Sci.* **2005**, *1062*, 209–219. [[CrossRef](#)]
35. Czura, C.J.; Tracey, K.J. Autonomic Neural Regulation of Immunity. *J. Intern. Med.* **2005**, *257*, 156–166. [[CrossRef](#)]
36. Tracey, K.J. Physiology and Immunology of the Cholinergic Antiinflammatory Pathway. *J. Clin. Investig.* **2007**, *117*, 289–296. [[CrossRef](#)]
37. Takata, K.; Amamiya, T.; Mizoguchi, H.; Kawanishi, S.; Kuroda, E.; Kitamura, R.; Ito, A.; Saito, Y.; Tawa, M.; Nagasawa, T.; et al. Alpha7 Nicotinic Acetylcholine Receptor-Specific Agonist DMXBA (GTS-21) Attenuates A β Accumulation through Suppression of Neuronal γ -Secretase Activity and Promotion of Microglial Amyloid- β Phagocytosis and Ameliorates Cognitive Impairment in a Mouse Model of Alzheimer's Disease. *Neurobiol. Aging* **2018**, *62*, 197–209. [[CrossRef](#)]
38. Medeiros, R.; Castello, N.A.; Cheng, D.; Kitazawa, M.; Baglietto-Vargas, D.; Green, K.N.; Esbenshade, T.A.; Bitner, R.S.; Decker, M.W.; LaFerla, F.M. A7 Nicotinic Receptor Agonist Enhances Cognition in Aged 3xTg-AD Mice with Robust Plaques and Tangles. *Am. J. Pathol.* **2014**, *184*, 520–529. [[CrossRef](#)]
39. Fucile, S.; Renzi, M.; Lax, P.; Eusebi, F. Fractional Ca²⁺ Current through Human Neuronal A7 Nicotinic Acetylcholine Receptors. *Cell Calcium* **2003**, *34*, 205–209. [[CrossRef](#)] [[PubMed](#)]
40. Shen, J.; Yakel, J.L. Nicotinic Acetylcholine Receptor-Mediated Calcium Signaling in the Nervous System. *Acta Pharmacol. Sin.* **2009**, *30*, 673–680. [[CrossRef](#)]
41. Fucile, S. Ca²⁺ Permeability of Nicotinic Acetylcholine Receptors. *Cell Calcium* **2004**, *35*, 1–8. [[CrossRef](#)] [[PubMed](#)]
42. Leiser, S.C.; Bowlby, M.R.; Comery, T.A.; Dunlop, J. A Cog in Cognition: How the A7 Nicotinic Acetylcholine Receptor Is Geared towards Improving Cognitive Deficits. *Pharmacol. Ther.* **2009**, *122*, 302–311. [[CrossRef](#)] [[PubMed](#)]
43. Hayward, A.; Adamson, L.; Neill, J.C. Partial Agonism at the A7 Nicotinic Acetylcholine Receptor Improves Attention, Impulsive Action and Vigilance in Low Attentive Rats. *Eur. Neuropsychopharmacol.* **2017**, *27*, 325–335. [[CrossRef](#)] [[PubMed](#)]
44. Dineley, K.T.; Pandya, A.A.; Yakel, J.L. Nicotinic ACh Receptors as Therapeutic Targets in CNS Disorders. *Trends Pharmacol. Sci.* **2015**, *36*, 96–108. [[CrossRef](#)]

45. Shytle, R.D.; Mori, T.; Townsend, K.; Vendrame, M.; Sun, N.; Zeng, J.; Ehrhart, J.; Silver, A.A.; Sanberg, P.R.; Tan, J. Cholinergic Modulation of Microglial Activation by A7 Nicotinic Receptors. *J. Neurochem.* **2004**, *89*, 337–343. [[CrossRef](#)]
46. De Jesus Moreno Moreno, M. Cognitive Improvement in Mild to Moderate Alzheimer’s Dementia after Treatment with the Acetylcholine Precursor Choline Alfoscerate: A Multicenter, Double-Blind, Randomized, Placebo-Controlled Trial. *Clin. Ther.* **2003**, *25*, 178–193. [[CrossRef](#)]

Disclaimer/Publisher’s Note: The statements, opinions and data contained in all publications are solely those of the individual author(s) and contributor(s) and not of MDPI and/or the editor(s). MDPI and/or the editor(s) disclaim responsibility for any injury to people or property resulting from any ideas, methods, instructions or products referred to in the content.